HKI-272 contributes to gemcitabine-mediated anti-proliferative and anti-metastatic effects through EGFR suppression in gallbladder cancer

Xuli Yang,[1,5] Tao Chen,[2,5] Jie Hu,[3] Jian Wang,[2] and Dong Yang[4]

[1]Department of Anesthesiology, Nanjing Drum Tower Hospital, The Affiliated Hospital of Nanjing University Medical School, Nanjing, Jiangsu 210008, China; [2]Department of Biliary-Pancreatic Surgery, Renji Hospital, School of Medicine, Shanghai Jiao Tong University, Shanghai 200127, China; [3]Department of Anesthesiology, The Second Affiliated Hospital of University of South China, Hengyang, Hunan 421001, China; [4]Department of Gastroenterology and Pancreatic Surgery, The Affiliated Jiangning Hospital with Nanjing Medical University, Nanjing, Jiangsu 211100, China

Gallbladder cancer (GBC) is a rare malignancy of the biliary system and characterized by early metastasis and poor prognosis. To date, no efficient treatment is available for GBC patients. Based on the data from cBioPortal, TIMER, and GDSC, we performed an unbiased screening with 25 candidate compounds that predominantly target ErbB family and identified HKI-272, a highly selective EGFR/ErbB2 inhibitor, displayed decreased IC$_{50}$ values in three GBC cell lines. HKI-272 not only promoted gemcitabine-mediated anti-proliferative and pro-apoptotic effects and induced cell cycle arrest in GBC, but also enhanced gemcitabine-induced suppressive effects of GBC cell migration and invasion by inhibiting pathways downstream of EGFR. Furthermore, HKI-272, together with gemcitabine, effectively suppressed tumor growth and metastases in mouse models. Immunostaining and HE staining data from both primary tumor and lung metastasis indicated that the anti-proliferative and anti-metastatic effects were mediated through EGFR suppression. Moreover, the expression of EGFR, measured by both immunostaining and HE staining, was correlated with a poor prognosis in GBC. In addition, EGFR in tumor tissues are independent indicators for overall survival in GBC patients. Taken together, our findings suggest that HKI-272 could be a potential therapeutic agent and EGFR might serve as a potential biomarker for patients with GBC.

INTRODUCTION

Gallbladder cancer (GBC) is a rare but highly lethal malignancy originating from the biliary system.[1,2] Owing to early hematogenous and lymphatic metastasis,[3] as well as direct liver invasion,[4] the prognosis is extremely dismal, with a 5-year survival rate of approximately 5%.[5] Evidence suggests that GBC patients with metastases are unable to benefit from radical surgery and thus systemic chemotherapy is recommended.[6] To date, gemcitabine remains the standard first-line chemotherapy regimen, although the median overall survival in only 7.7 months.[7] Unfortunately, second-line chemotherapeutic drugs in GBC patients are not available.[8] However, it was reported that patients with GBC may benefit from gemcitabine-based treatments.[9] Hence, the identification of effective drugs that might enhance gemcitabine sensitivity is pivotal in the treatment of GBC.

The ErbB receptor family is composed of the epidermal growth factor receptor (EGFR) or ErbB1/Her1, ErbB2/Her2, ErbB3/Her3, and ErbB4/Her4.[10] Analyses of whole-exome sequencing data have revealed that ErbB pathway mutations are crucial in the regulation of GBC malignancy.[11,12] In addition, a number studies have shown that the dysregulation of ErbB pathways is strongly correlated with metastases in various cancers.[13–15] By screening small molecule libraries that target the ErbB pathway in GBC cells, our early study confirmed that the inhibition of mammalian target of rapamycin (mTOR), which is downstream of ErbB/PI3K pathway,[16,17] represents a potential therapeutic by effectively suppressing tumor growth and metastasis in GBC.[18] However, a comprehensive screening by small molecule inhibitors that predominantly target ErbB family in GBC is still lacking.

In the current study, we performed a supplemental screening with 25 compounds that predominantly target EGFR, ErbB2, ErbB3, and ErbB4. These compounds are selected based on at least one of the criteria below: (1) They were derived from the Genomics of Drug Sensitivity in Cancer (GDSC) database and showed satisfactory anti-tumor effect. (2) They displayed decreased half-maximal inhibitory concentration (IC$_{50}$) values among other cancer types. (3) They have already been enrolled in clinical trials. Finally, we identified HKI-272, a highly selective EGFR/ErbB2 inhibitor, which has been
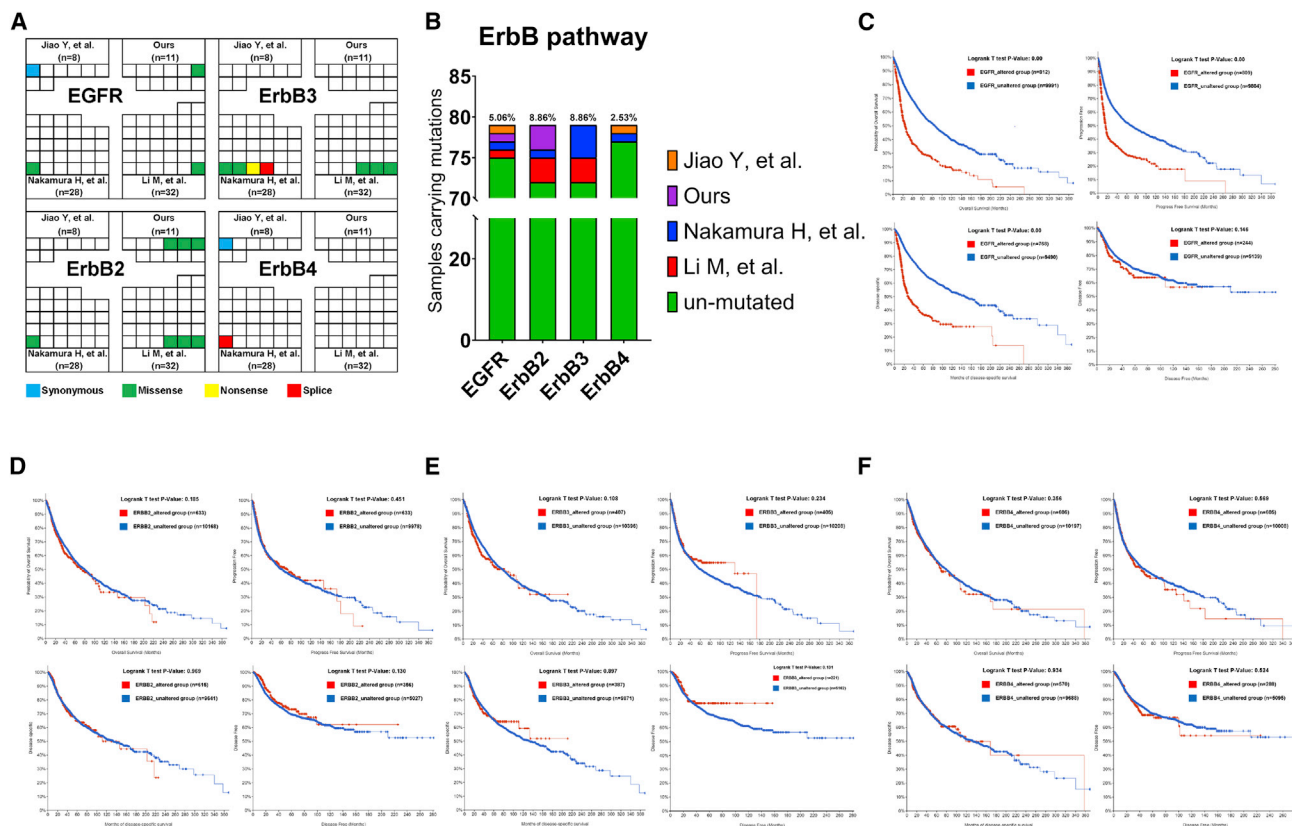
Figure 1. Analysis of GBC mutation and survival of EGFR/ErbB2/ErbB3/ErbB4

(A) Number of GBC samples from ErbB family members harboring 4 common mutation types (synonymous, missense, nonsense and splice) were indicated. (B) The total mutation ratio of EGFR, ErbB2, ErbB3, and ErbB4 from four GBC sources. (C–F) Pan-cancer comparison of OS, PFS, DSS, and DFS between patients with altered and unaltered mutations of EGFR/ErbB2/ErbB3/ErbB4 using cBioPortal database.

widely introduced in clinical trials for treating ErbB2-positive meta-static breast cancer,[19–21] and displayed remarkable anti-proliferative and anti-metastatic effects in GBC. Furthermore, the chemosensitivity of GBC cells to gemcitabine was also markedly magnified by HKI-272 both *in vitro* and *in vivo*. In addition, EGFR in tumor tissues is an independent indicator for overall survival in GBC patients. However, HKI-272 and its effectiveness have not been studied in GBC so far, let alone its application to clinical trial. Taken together, our findings suggest that HKI-272 could serve as a potential therapeutic agent and EGFR might serve as a potential biomarker for patients with GBC.

RESULTS

Genes in ErbB family are highly mutated in GBC samples

Our early publication revealed that genes in the ErbB/PI3K/Akt/mTOR pathway were frequently mutated.[18] In the present study, we denoted four specific mutation types (synonymous, missense, nonsense, and splice) in 79 GBC samples that were derived from our data and three other sources[11,12,22] (Figure 1A). The mutation ratios of EGFR, ErbB2, ErbB3, and ErbB4 were 5.06%, 8.86%, 8.86%, and 2.53%, respectively (Figure 1B). We noticed that the mutation ratio of ErbB family is much higher than other genes downstream of the

ErbB pathway. Furthermore, a pan-cancer survival analysis from the cBioPortal database suggested that overall survival (OS), progression-free survival (PFS), and disease-specific survival (DSS) in EGFR-mutated patients were all markedly shortened (Figure 1C). However, disease-free survival (DFS) remained unchanged between the EGFR-mutated and EGFR-unmutated groups (Figure 1C). Interestingly, no difference in OS, PFS, DSS, or DFS was observed in patients with or without mutations in ErbB2, ErbB3, or ErbB4 (Figures 1D–1F). These results indicated that EGFR might be crucial for oncogenesis and prognosis in patients with GBC.

Exploration of expression and drug efficacy of EGFR from pan-cancer analyses

Expression analysis of a serial of tumors and adjacent non-tumor tissues from the tumor immune estimation resource (TIMER) database revealed that EGFR expression was extensively dysregulated across multiple malignancies, which emphasized a potential therapeutic role for EGFR in GBC (Figure 2A). We reported that mTOR inhibitor INK-128 might be a potential therapeutic in GBC.[18] In the present study, we sought to identify compounds that predominantly target the ErbB family and validate their anti-tumor effects. The drug
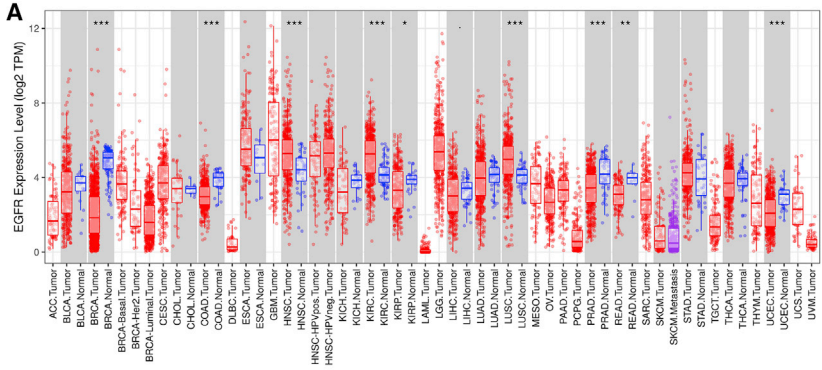
A

Figure 2. Pan-cancer analysis of EGFR expression and IC50 values of compounds targeting EGFR

(A) Differential expression of EGFR among a serial of tumors and adjacent normal tissues from TIMER database. (B) IC50 values of compounds in multiple tumors harboring EGFR mutation. These data were derived from GDSC database. (C) AZD3759, osimertinib, gefitinib (GDSC2 dataset), and afatinib (GDSC1 dataset) demonstrated decreased IC50 values and strong anti-tumor effects in EGFR-mutated cancer cells. (D) IC50 values of AZD3759 among a series of malignancies. GBC cells are not included in the GDSC database.

B

C

D

A

B

C G+H for SGC-996

D G+H for GBC-SD

E G+H for NOZ
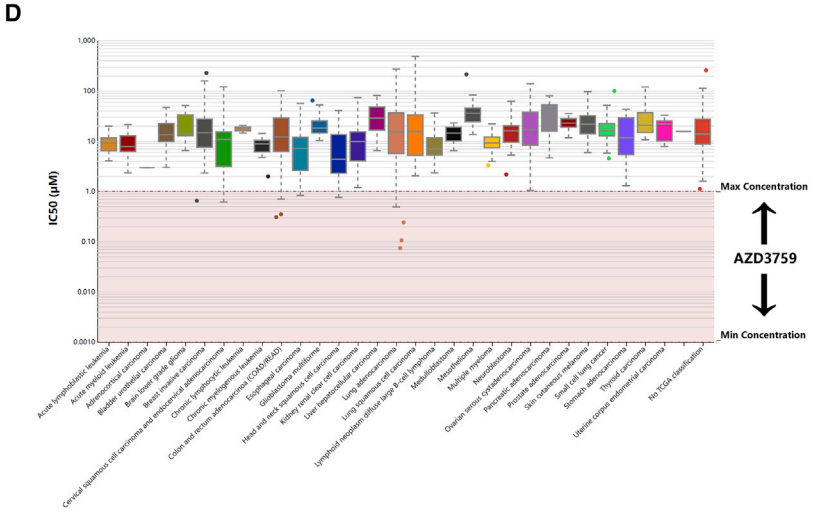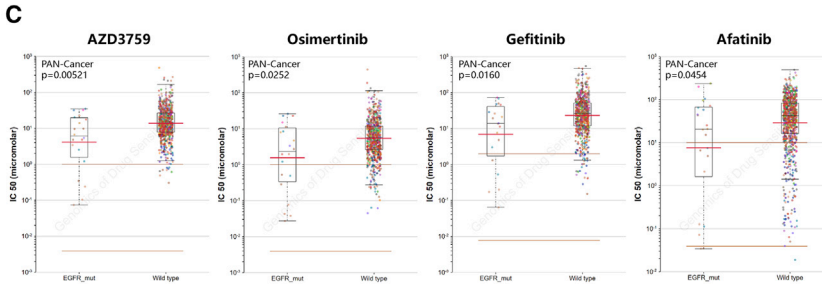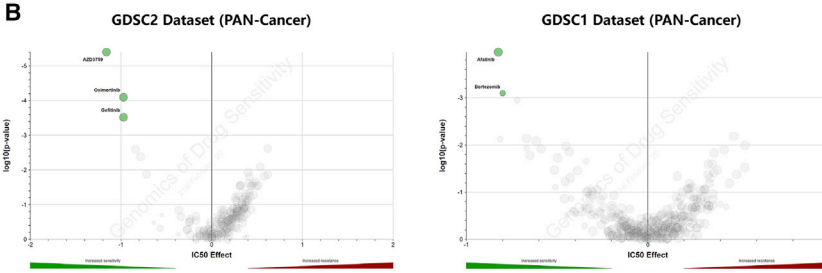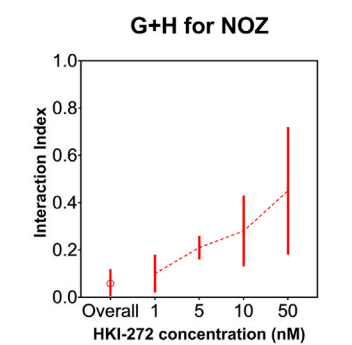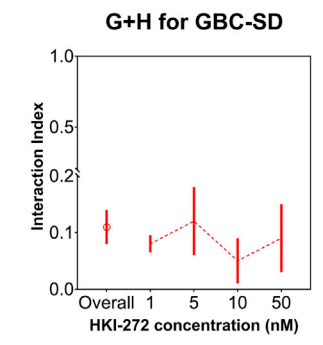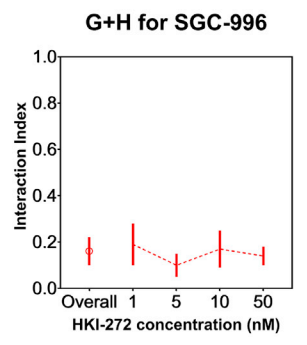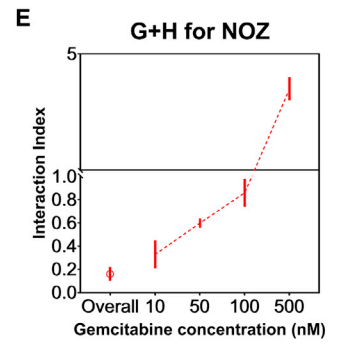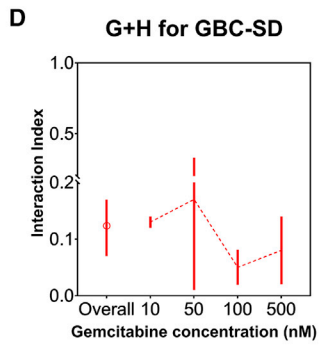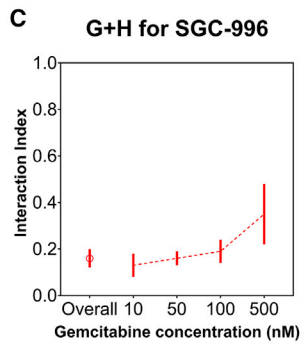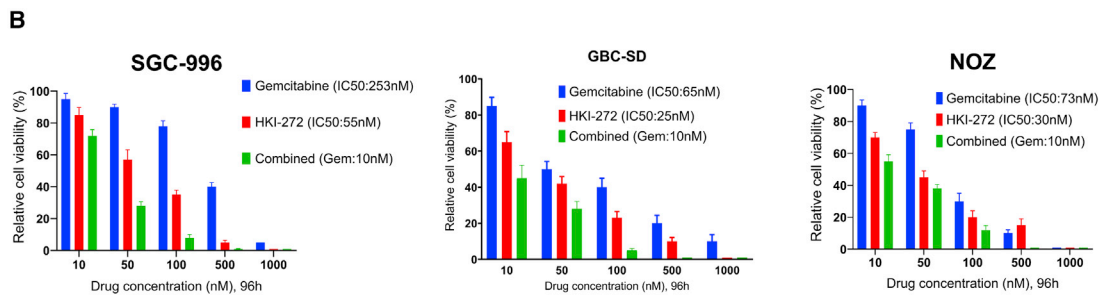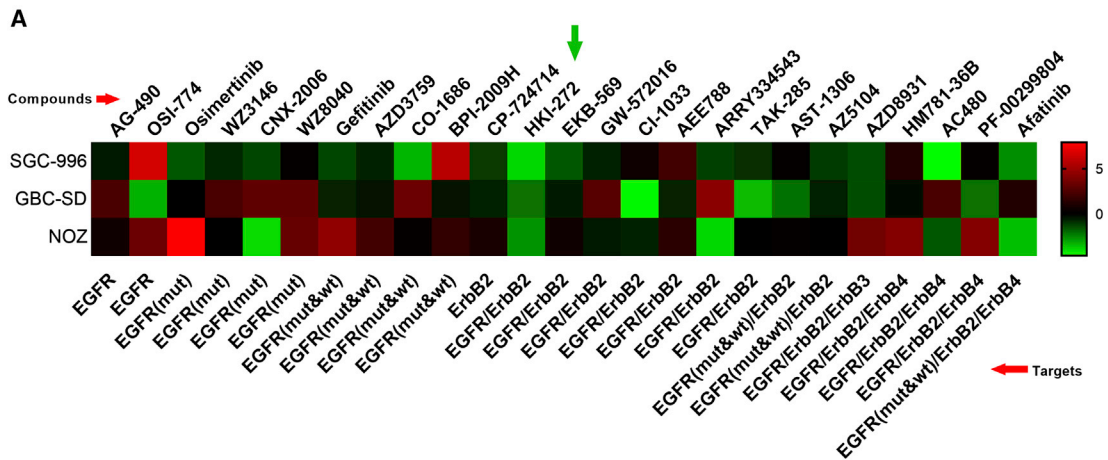
(legend on next page)

screening data from GDSC showed that AZD3759, osimertinib, gefitinib (from the GDSC2 dataset), and afatinib (from the GDSC1 dataset) displayed a decreased IC_{50} value in multiple tumors harboring EGFR mutation (Figures 2B and 2C). The difference between dataset GDSC2 and GDSC1 is illustrated in the materials and methods. Bortezomib, another effective candidate from GDSC1, was excluded owing to its proteasome inhibitor property. In contrast, no compound in the GDSC database was identified to efficiently target ErbB2, ErbB3, or ErbB4 (data not shown), which indicated that EGFR, when compared with other ErbB family members, might be a promising therapeutic in GBC patients. Notably, AZD3759 outscores other EGFR inhibitors with a distinguished IC_{50} effect size among a series of malignancies (Figure 2D). However, no GBC cell lines were enrolled or investigated in the GDSC database and little literature is available on whether these compounds that target are effective in GBC. Taken together, these results suggested that a compound library that target ErbB family (EGFR, ErbB2, ErbB3, or ErbB4) for identifying potential therapeutics is required in GBC.

Screening of small molecule compounds targeting ErbB family members

To further identify the potential molecular vulnerabilities in GBC, we conducted a screening using a total of 25 compounds that predominantly target ErbB family in vitro. The inclusion criteria had been depicted in the Introduction. We noticed that HKI-272, a highly selective EGFR/ErbB2 inhibitor with decreased IC_{50} values, exhibited robust anti-proliferative effects in all three GBC cell lines (Figure 3A). As compared with the traditional chemotherapeutic gemcitabine, HKI-272 significantly suppresses tumor cell growth in a dose-dependent manner (Figure 3B). Although gemcitabine at 10 nM alone was unable to effectively inhibit cell growth, HKI-272 combined with 10 nM gemcitabine demonstrated a dose-dependent anti-proliferative effect in SGC-996, GBC-SD, and NOZ cells (Figure 3B). To explore whether HKI-272 synergizes with gemcitabine in suppressing GBC growth, a dose-response surface model based on the Bliss independence principle was applied to GBC cells treated with combinations of various doses of these drugs. The interaction index and its 95% confidence interval (CI) were calculated to evaluate a two-drug combination effect.[23,24] An index score of less than 1 indicates synergy. As expected, the combination of HKI-272 and gemcitabine demonstrated a synergistic effect compared with single drug use in SGC-996, GBC-SD, and NOZ cells (Figures 3C–3E). Taken together, these data indicated that HKI-272 might serve as a potential therapeutic agent and potentiated GBC cells sensitivity to gemcitabine in GBC.

HKI-272 promoted gemcitabine-mediated anti-proliferative and pro-apoptotic effects and induced cell cycle arrest in GBC

We introduced a colony formation assay to further assess the anti-proliferative effect of HKI-272 on human GBC cells. As shown in Figure 4A, the colony formation rate of SGC-996, GBC-SD, and NOZ were decreased significantly when treated with gemcitabine, and this anti-proliferative effect was potentiated by HKI-272. Moreover, annexin V/propidium iodide (PI) double staining assay was used to evaluate the cell apoptosis rate induced by HKI-272 and/or gemcitabine. Marked cell apoptosis was observed in the HKI-272 plus gemcitabine group compared with the single drug group (Figure 4B). Immunoblotting was introduced to measure the expression of BCL-2, a classic anti-apoptotic marker, in these cells mentioned above. We discovered that BCL-2 expression was significantly decreased when both HKI-272 and gemcitabine were administrated (Figure 4C). To evaluate the effects of HKI-272 and/or gemcitabine on the regulation of the cell cycle, DNA content was measured by flow cytometry. Treatment of HKI-272 alone resulted in a decrease of the G0/G1 phase, and an increase of the synthesis phase. Meanwhile, the combined treatment (HKI-272 plus gemcitabine) displayed a significant increase in the proportion of cells in the synthesis phase and a decrease in the G0/G1 phase. However, we noticed that HKI-272 promoted gemcitabine-induced G2/M phase inhibition only in two cell lines, GBC-SD and NOZ (Figure 4D). Taken together, HKI-272 promoted gemcitabine-induced anti-proliferation, pro-apoptosis, and cell cycle arrest in GBC cells.

HKI-272 enhanced gemcitabine-induced suppressive effects of cell migration and invasion by inhibiting pathways downstream of EGFR in GBC

To elucidate whether HKI-272 or/and gemcitabine play a role in regulating cell migration and invasion in GBC, we investigated the migration ability and invasiveness in three GBC cells treated with DMSO, gemcitabine, HKI-272, or gemcitabine plus HKI-272. As shown in Figures 5A and 5B, both migration ability and invasiveness were weakened by gemcitabine or HKI-272 alone, while HKI-272 combined with gemcitabine exhibited a more powerful effect in repressing migration and invasion in GBC cells. Moreover, the EGFR/PI3K pathway was reported to participate in tumorigenesis, invasion, and distant metastasis in various cancers.[25–28] Our recent study also confirmed that the activation of mTOR is correlated with poor prognosis and is an independent marker for poor survival in GBC patients.[18] Under these circumstances, we investigated the EGFR/PI3K-related protein levels in GBC cells that were subjected to different treatments. In line with the results from cell proliferation, apoptosis, and mobility assays, either HKI-272 or gemcitabine inhibited the expression of phosphorylated EGFR, PI3K, Akt, mTOR, and ERK1/2, while the co-administration of HKI-272 and gemcitabine demonstrated a more robust inhibitory effect in suppressing EGFR signaling (Figure 5C). These data indicated that HKI-272 was able to potentiate the anti-migratory and anti-invasion effects induced by gemcitabine by down-regulating the expression of EGFR and its downstream targets.

Figure 3. IC_{50} values of compounds targeting the ErbB family in GBC

(A) Heatmap of IC_{50} value of compounds targeting the ErbB family. Compound names and their targets are indicated with red arrows. HKI-272, a highly selective EGFR/ErbB2 inhibitor, exhibited robust decreased IC_{50} values in all three GBC cell lines. (B) Validation of anti-proliferative effects of HKI-272 or/and gemcitabine in three GBC cells. The IC_{50} values of each drug in each cell line were also demonstrated. (C–E) Synergistic anti-proliferative effects of HKI-272 and gemcitabine in three GBC cells.
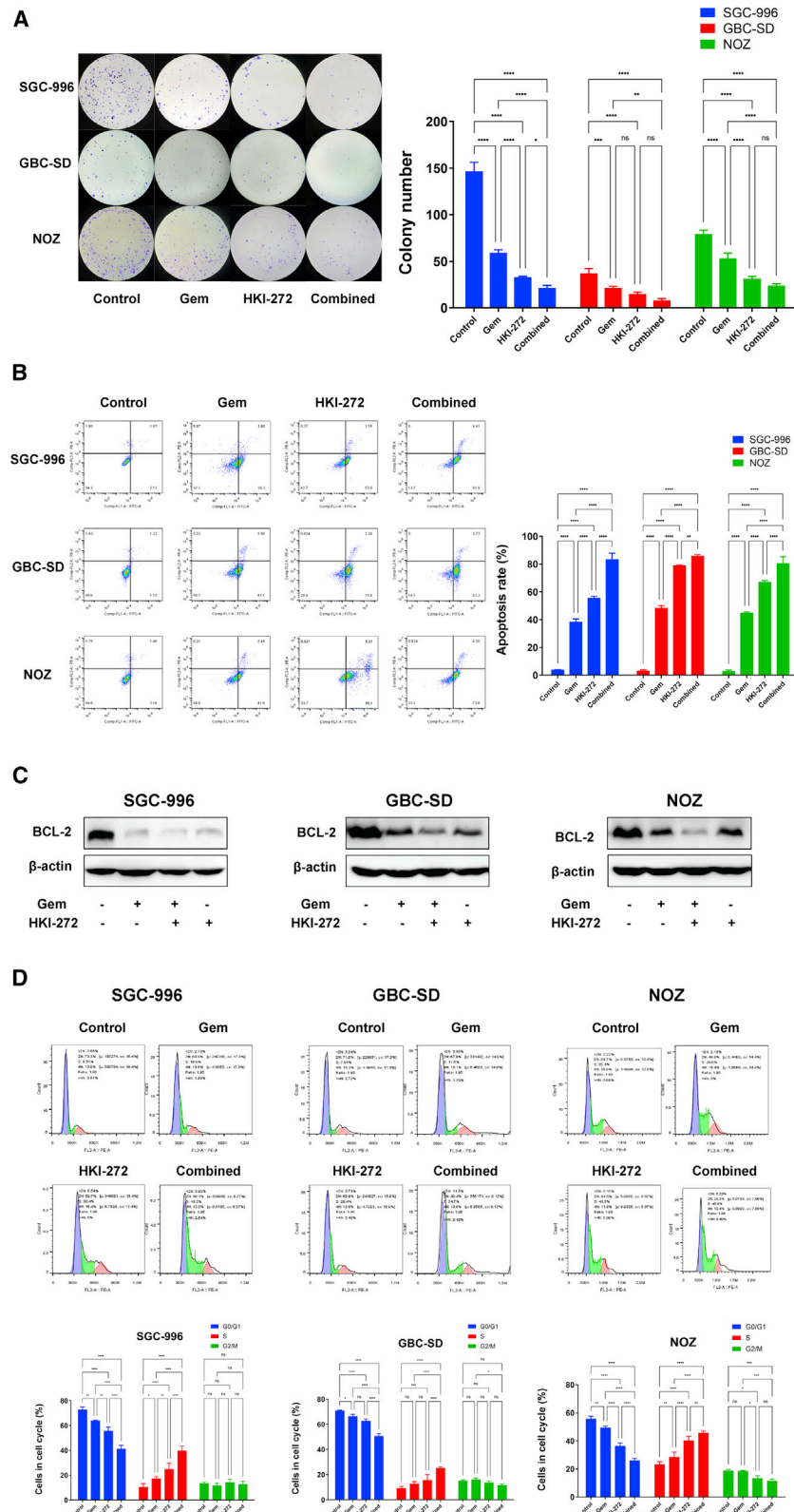
Figure 4. HKI-272 repressed cell colony formation, induced cell apoptosis, and caused cell cycle arrest *in vitro*

(A) Representative images of colonies in SGC-996, GBC-SD, and NOZ cells that were treated with DMSO, gemcitabine, HKI-272, or a mixture of gemcitabine and HKI-272. Quantifications of the colony formation rate were also evaluated. (B) HKI-272 increased apoptotic sensitivity to gemcitabine treatment in GBC cells. Apoptosis rates were measured using annexin V/PI staining. (C) BCL-2 protein expression was detected by immunoblotting in three GBC cells. (D) HKI-272 promoted gemcitabine-induced S phase arrest in SGC-996, GBC-SD, and NOZ. Cell cycle distribution was visualized in GBC cells exposed to DMSO, gemcitabine, HKI-272 or a combination of gemcitabine and HKI-272. Quantifications of the phase population percentage were also indicated. Data were shown as mean ± standard error of the mean of three independent experiments and ANOVA was used to calculate p value. $*p < 0.05$; $**p < 0.01$; $***p < 0.001$; $****p < 0.0001$; n.s., not significant.

A

B

C
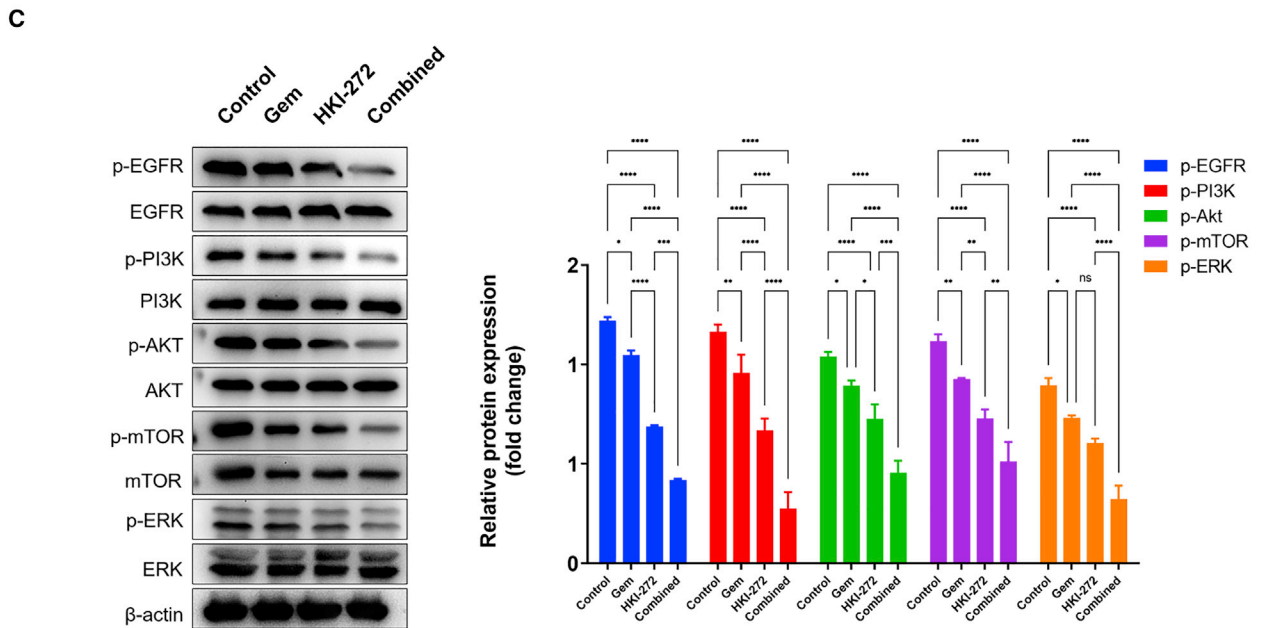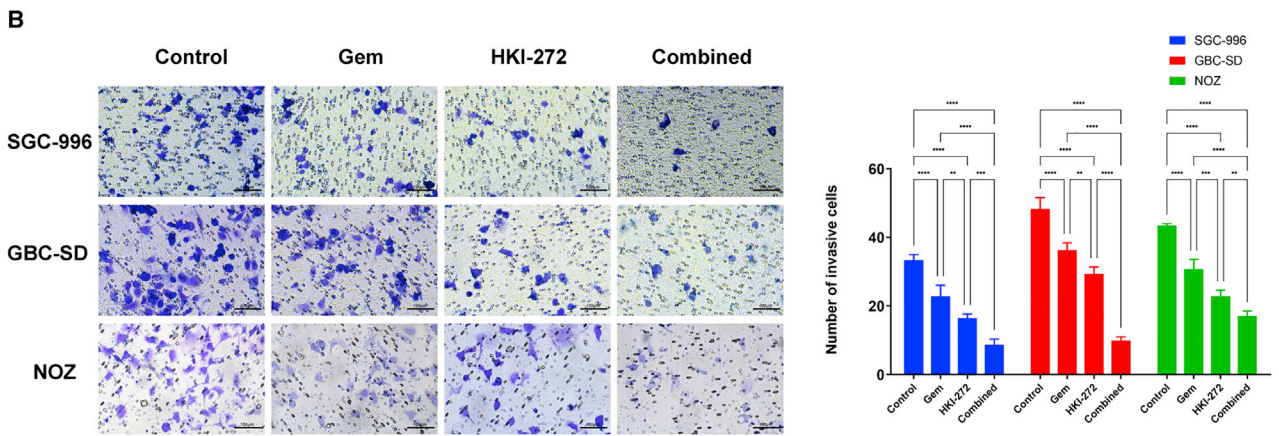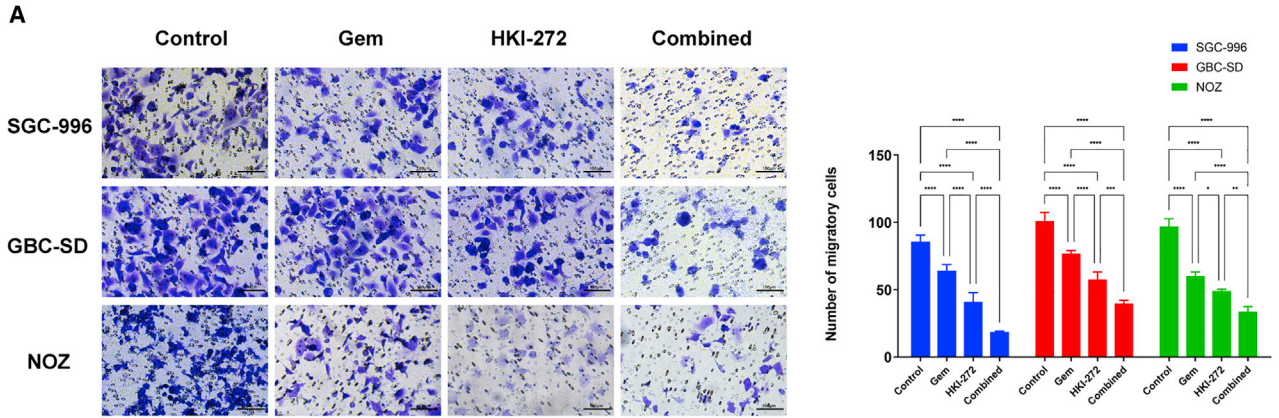
(legend on next page)

HKI-272 potentiates gemcitabine-mediated anti-proliferative and anti-metastatic effects via the suppression of EGFR *in vivo*

To further investigate the efficacy of HKI-272 on a xenograft model, luciferase-tagged GBC-SD cells were subcutaneously transplanted, based on our earlier study.[18] DMSO, gemcitabine, HKI-272, or gemcitabine plus HKI-272 were then separately administrated. Tumor volume was measured with an external caliper weekly to determine tumor growth. Our results suggested that tumor growth was significantly inhibited in terms of tumor volume and bioluminescent flux. Lung metastasis was detected in four of five mice treated with gemcitabine alone. However, HKI-272 not only suppressed tumor growth, but also mitigated metastasis (1/5 mice) as compared with either the control or gemcitabine groups. Surprisingly, we noticed that no lung metastasis was developed in the dual drug group. Furthermore, body weight among the four groups remained unchanged at week 6 (Figure 6B), suggesting that all drugs and their combination were tolerable in mice. Afterward, primary tumors and lung metastases were carefully dissected out and pathologically confirmed as cancer tissue, followed by EGFR expression detection with both immunostaining and hematoxylin and eosin (HE) staining. As demonstrated in Figures 6C and 6D, EGFR expression was decreased in both primary and metastatic tumor samples in mice administrated gemcitabine or HKI-272 alone. Furthermore, we noticed a significantly weakened EGFR expression when HKI-272 and gemcitabine were given together. Taken together, these results suggested that gemcitabine-mediated anti-proliferative and anti-metastatic effects were potentiated by HKI-272 via suppression of EGFR in animal models.

EGFR is negatively correlated with post-surgical survival in GBC patients

We have demonstrated that the inhibition of EGFR by HKI-272 resulted in robust anti-tumor effects in GBC. Because EGFR is the trigger for a variety of downstream oncogenic pathways, it is convincing that GBC patients' survival is inversely regulated by EGFR activation. Representative images of high-level and low-level EGFR expressions in postoperative tumor samples were demonstrated using both immunostaining and HE staining (Figures 7A and 7B). As compared with the high EGFR expression group, patients with low EGFR expression exhibited a longer life expectancy after surgery (Figure 7C). Multivariable analyses revealed that EGFR can serve as an independent marker of survival (Table 1). These data indicated that high EGFR expression was correlated with a poor prognosis and targeted therapy to EGFR might be beneficial to GBC patients. To identify potential genes and proteins that interacted with EGFR, we constructed the gene-gene interaction network for EGFR to filter possible impacted genes using the GeneMania database (Figure 7D).
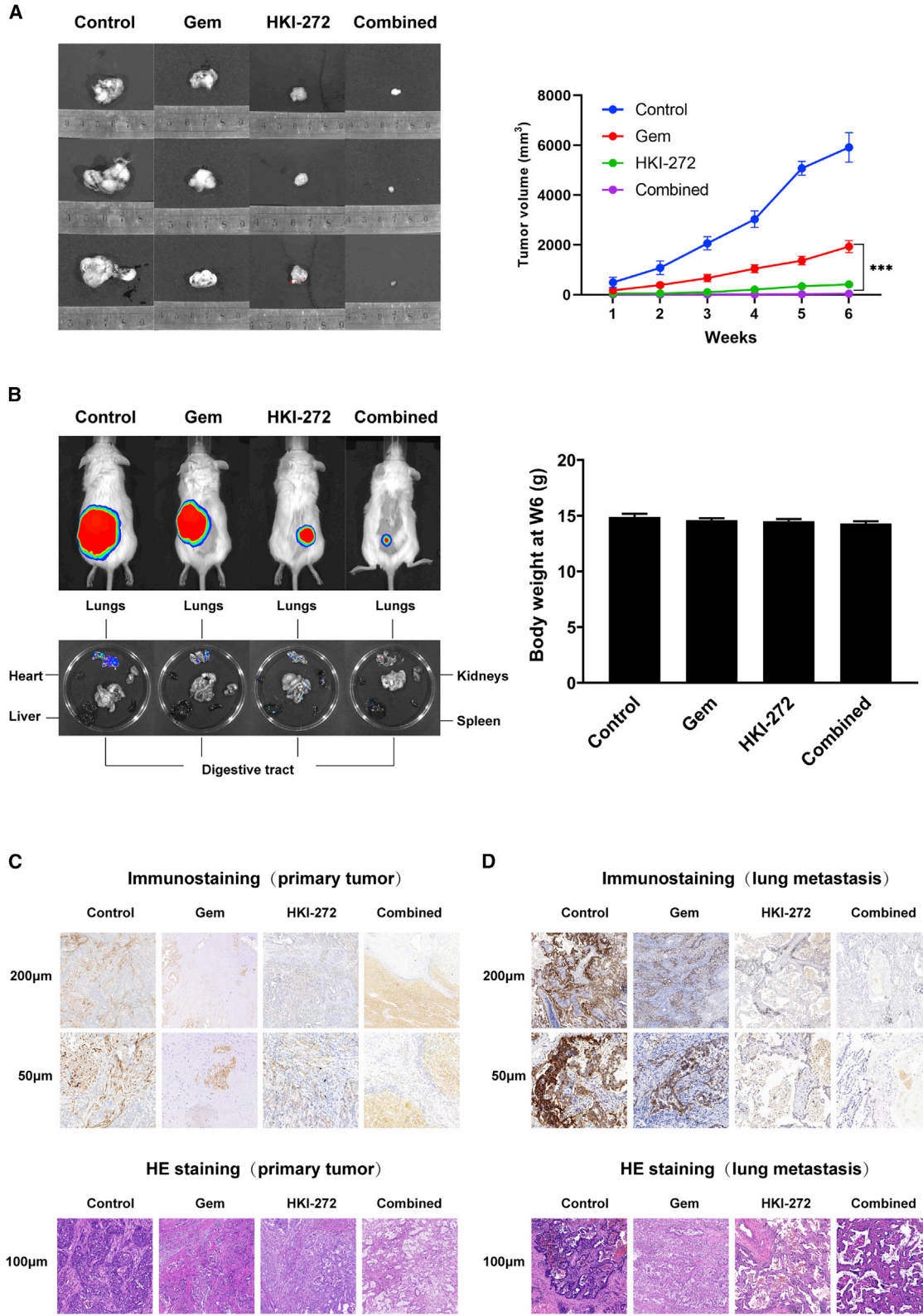
The top 20 altered genes were closely associated with EGFR, including PIK3CA,[29,30] ADAM12,[31] and ANXA2,[32] which were involved in GBC and breast cancer. This network is predominantly composed of physical interaction (77.64%, pink lines) followed by co-expression (8.01%, purple lines) and prediction (5.37%, yellow lines). To gain full insight into EGFR interactions at protein level, STRING database was introduced to generate a protein-protein interaction (PPI) network. A total of 11 nodes and 42 edges are included here (Figure 7E). HBEGF, PLCG1, and EREG are displayed as top predicted functional partners. Taken together, these data paved the way for further identification of potential therapeutical targets in GBC.

DISCUSSION

GBC is an uncommon but highly life-threatening malignancy with no current effective medications.[33–35] Our previous work demonstrated that ErbB family members and the downstream targets were highly mutated, and mTOR, which is impressively inhibited by INK-128, might be a potential therapeutic target in GBC.[18] Unfortunately, EGFR, ErbB2, ErbB3, and ErbB4 were not fully included in our early compound library. In the present study, we first referred to the GDSC database and found that AZD3759, along with three other compounds, exhibit decreased IC_{50} values in a variety of malignancies harboring EGFR mutations. However, no efficient drug targeting ErbB2, ErbB3, or ErbB4 was found in GDSC. Second, a pan-cancer analysis from cBioPortal suggested that OS, PFS, and DSS are decreased only in EGFR-mutated patients, suggesting that EGFR might be a potential therapeutic target. Furthermore, traditional gemcitabine-based chemotherapy has been unsatisfactory in treating GBC.[7,36] In contrast with the GDSC data suggesting that EGFR inhibitors including AZD3759 exhibited a low IC_{50} effect size among a series of malignancies, our screening results indicated that HKI-272 outscored other ErbB family inhibitors including AZD3759 with conspicuously decreased IC_{50} values in all three GBC cells. Although AZD3759 demonstrated even lower IC_{50} values in SGC-996 and GBC cell lines as compared with HKI-272, it was unable to effectively suppress NOZ. Hence, we selected HKI-272 for further validation. HKI-272, which predominantly targets EGFR and ErbB2, not only sensitizes GBC cells to gemcitabine in inhibiting cell growth, inducing cell apoptosis, and cell cycle arrest, but also promoted the gemcitabine-mediated suppression of cell migration and invasion. Western blot analysis indicated that the anti-proliferative, anti-metastatic, and pro-apoptotic effects of HKI-272 were regulated by the inhibition of the EGFR/PI3K pathway in GBC. In addition, HKI-272 synergized with gemcitabine in suppressing primary tumor growth and lung metastasis in mouse models. Importantly, no body weight change was observed among the mice subject to various remedies (DMSO,

Figure 5. HKI-272 facilitated gemcitabine-induced inhibition of cell migration and invasion by suppressing pathways downstream of EGFR in GBC

SGC-996, GBC-SD, and NOZ cells were divided into four groups: DMSO, gemcitabine, HKI-272, and combination of gemcitabine and HKI-272. (A, B) Cell migration ability and invasiveness were detected by using trans-well chambers. The numbers of migrated and invaded cells were also demonstrated. (C) Expression of EGFR, PI3K, Akt, mTOR, and ERK was analyzed by western blotting in GBC cells with β-actin as the loading control. Quantifications of the gray-scale value of straps were also shown. Data were shown as mean ± standard error of the mean of three independent experiments and ANOVA was used to calculate the p values. *p < 0.05; **p < 0.01; ***p < 0.001; ****p < 0.0001; n.s., not significant.

A

B

C Immunostaining（primary tumor）

HE staining（primary tumor）

D Immunostaining（lung metastasis）

HE staining（lung metastasis）

(legend on next page)

HKI-272, gemcitabine, or HKI-272 plus gemcitabine), which indicated that these drugs are tolerable. Using both immunostaining and HE staining, we also detected EGFR expression on xenograft tumors, mice lung metastatic nodules, and human GBC samples. On the whole, these data revealed that HKI-272 markedly promoted gemcitabine-mediated inhibitory effects on tumor growth and metastasis and therefore a potential role of HKI-272 in the treatment of GBC (especially those resistant to standard first-line chemotherapeutic gemcitabine) is promising.

In this study, we showed that EGFR inhibition mediated by gemcitabine was remarkably enhanced by HKI-272 in animals and, moreover, that EGFR activation is inversely correlated with survival in GBC patients. Our early study shows that INK-128, a dual mTORC1/2 inhibitor, suppress cell growth and distant metastasis *in vitro* and *in vivo*. Furthermore, high expression of p-mTOR or p-S6K1 was negatively correlated with patients' prognosis and p-mTOR and p-S6K1 can serve as independent markers of survival.[18] Since HKI-272 have entered a serial of clinical trials on HER2-positive metastatic breast cancer patients,[19,20] we speculate whether a synergistic anti-tumor effect could be achieved by combining HKI-272 to INK-128 in the treatment of GBC. The combination anti-tumor effect, the optimal dosage of each drug, the tolerability in animal models, and whether a triple drug remedy (HKI-272 + INK-128 + gemcitabine) is practical will be further evaluated in our research.

To date, no literature regarding the application of HKI-272 to GBC is available, either in pre-clinical or clinical studies. Recently a targeted sequencing for gene mutations in 206 patients with non-small cell lung cancer (NSCLC) was undertaken.[37] The top three high-frequency mutation genes were TP53 (48%), EGFR (42%), and CREBBP (23%). Moreover, missense mutations represent the top mutation types in EGFR, which is in line with our current study. Given that EGFR inhibitors have been under evaluation in clinical trials for EGFR-mutated NSCLC patients,[38–40] we speculate whether HKI-272 could be applied clinically. Because a majority of patients are diagnosed at a late stage and are unsuitable for radical surgical resection, we proposed that these patients could be stratified by EGFR expression level via biopsy or circulating tumor cell collection. Patients with high EGFR expression will be potentially druggable. Even for those with low EGFR expression, a second stratification for high mTOR expression is our alternative choice. With the dual expression stratification system (high EGFR or high mTOR expression or both), the number of patients who might benefit is potentially increased. Our findings will shed light on the development and modification of new, more effective and less toxic drugs such as HKI-272, which target ErbB pathway as therapeutics in GBC patients.

MATERIALS AND METHODS

cBioPortal database
The cBioPortal for Cancer Genomics (https://www.cbioportal.org/) provides access to a large-scale cancer genomics dataset and serve as a powerful tool for downloading, analyzing and visualization.[41,42] We analyzed the OS, PFS, DSS, and DFS of ErbB family members (EGFR, ErbB2, ErbB3, and ErbB4) separately through the "Comparison/Survival" module.

The TIMER database
The TIMER database (https://cistrome.shinyapps.io/timer/) is an interactive portal that can be used for the molecular characterization of tumor-immune interactions.[43] It also allows users to investigate the differential expression between tumor and adjacent normal tissues for genes across TCGA. In the present study, we assessed EGFR expression in multiple types of cancer through the "Diff Exp" module.

The GDSC database
The GDSC database (https://www.cancerRxgene.org/) is the largest public resource for information on drug sensitivity in multiple cancer cell lines and molecular markers of drug response.[44] Two datasets—GDSC1 and GDSC2—are contained in GDSC. Data from 2010 to 2015 are included in GDSC1 and data from 2016 to present are included in GDSC2. We searched the GDSC for compounds that demonstrate decreased IC_{50} values in EGFR-mutant cell lines. The effectiveness of drugs is shown in the form of volcano plot, scatter plot and box plot. The Mann-Whitney-Wilcoxon tests were generated and computed via the GDSC online system.

GeneMANIA and STRING database
The GeneMANIA database (http://www.genemania.org/) is a user-friendly web interface for generating hypotheses about gene function, analyzing gene lists, and prioritizing genes for functional assays.[45] STRING (https://string-db.org/) aims to integrate all known and predicted associations between proteins, including both physical interactions as well as functional associations.[46] In the current study, GeneMANIA and STRING database were introduced to generate a gene-gene interaction and a PPI network of EGFR, respectively.

Cell culture and chemicals
Two human GBC cell lines, NOZ and GBC-SD, were maintained in Dulbecco's modified Eagle's medium. Another human GBC cell line, SGC-996, was maintained in RPMI-1640 medium, with all media containing 10% fetal bovine serum and antibiotics (Gibco, Grand Island, NY). Cells were maintained at 37°C in a humidified

---

Figure 6. HKI-272 suppressed GBC growth and metastasis in mouse models

Human GBC-SD cells tagged with luciferase were transplanted subcutaneously in mice from four groups: DMSO control, gemcitabine, HKI-272, or gemcitabine combined with HKI-272. (A) Tumor size was measured using an external caliper weekly. Tumor growth was significantly suppressed in mice treated with HKI-272 plus gemcitabine, as compared with mice subject to a single drug. (B) Tumor growth and lung metastasis were measured by a luminescence Xenogen system. Representative images of primary tumor and lung metastasis from one of five mice per group were demonstrated. Body weight was obtained at week 6 for all groups of mice. Immunohistochemistry and HE staining were conducted to determine EGFR expression in both primary tumors (Figure 6C) and lung metastasis (Figure 6D).

A

Immunostaining (clinical)
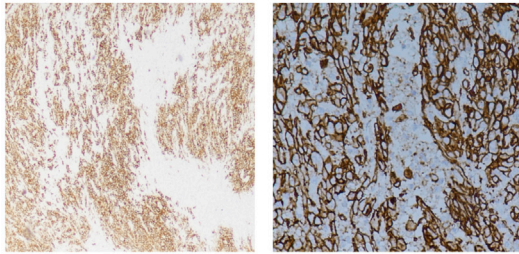
High EGFR 40×
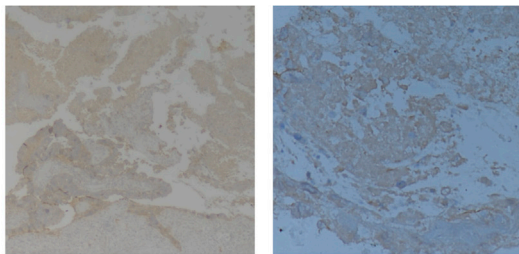
High EGFR 200×

Low EGFR 40×

Low EGFR 200×

B

HE staining (clinical)

High EGFR 40×
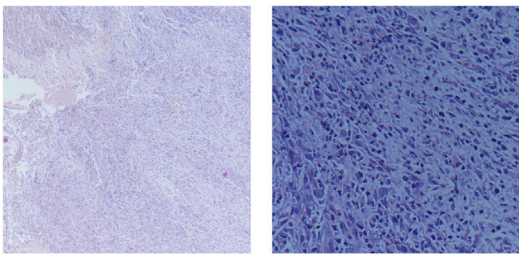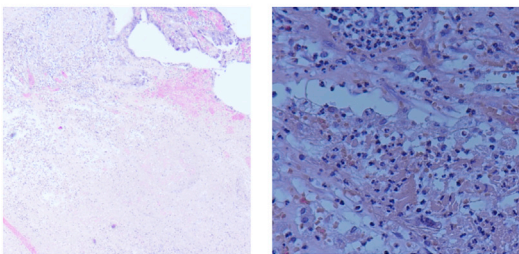
High EGFR 200×
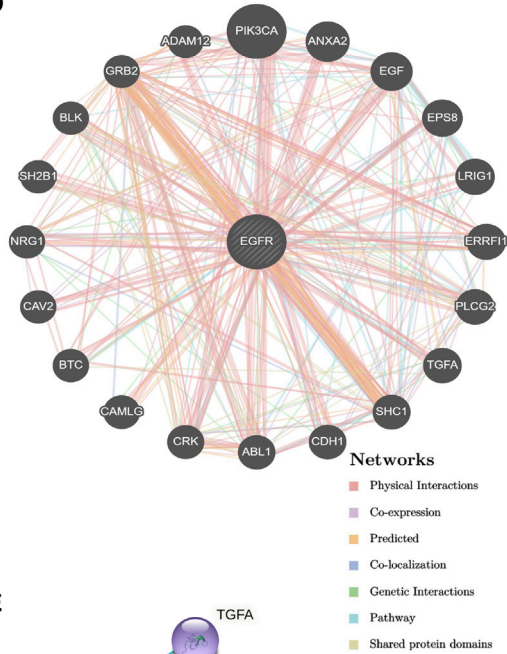
Low EGFR 40×

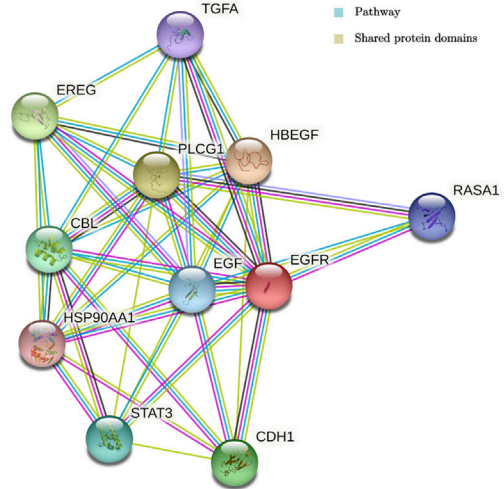**Low EGFR 200×**

C
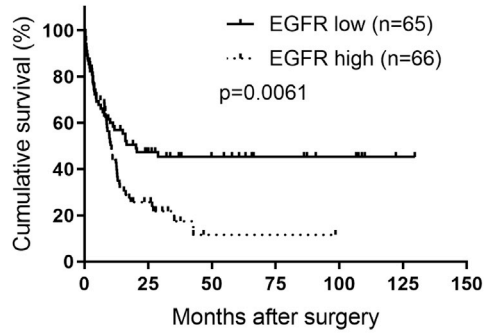
D

E

(legend on next page)

Table 1. Univariate and multivariable analysis of clinical characteristics influencing OS in GBC patients

Characteristics	Univariate analysis		Multivariate analysis	
	p Value	HR (95% CI)	p Value	HR (95% CI)
Gender (female vs. male)	0.120	1.40 (0.91–2.30)	0.331	0.80 (0.50–1.26)
Age (≥60 y vs. <60 y)	0.326	1.25 (0.79–2.07)	0.795	1.07 (0.66–1.71)
Tumor differentiation (well vs. moderate, poor or undifferentiated)	0.019	0.63 (0.40–0.92)	0.234	0.78 (0.52–1.18)
Tumor size (≥4 cm vs. <4 cm)	<0.001	0.50 (0.32–0.71)	0.132	0.71 (0.45–1.11)
TNM stage (0-II vs. III-IV)	<0.001	0.39 (0.25–0.56)	0.002	0.48 (0.30–0.76)
EGFR (low vs. high)	0.008	0.58 (0.43–0.88)	0.045	0.61 (0.40–0.82)

atmosphere consisting of 5% CO_2. NOZ was purchased from the Health Science Research Resources Bank (Osaka, Japan). GBC-SD and SGC-996 cells were provided by the Academy of Life Sciences, Tongji University (Shanghai, China). Gemcitabine, HKI-272 and 24 other compounds were purchased from Apex-Bio (Houston, TX).

Screening of small molecule inhibitors library and cell viability assay

To identify ErbB pathway inhibitors that suppressed the growth of GBC *in vitro*, a library of 25 small molecule inhibitors targeting EGFR, ErbB2, ErbB3m or ErbB4 were screened in SGC-996, GBC-SD, and NOZ cells. (Compound names and CIDs on PubMed are listed in Table S1). Cell viability was determined following 5 days' incubation in the presence of compounds. For each compound, a serial dilution (20 mM, 4 mM, 0.8 mM, 0.16 mM, 0.032 mM, 6.4 nM, 1.28 nM, 0.256 nM, 0.0512 nM, and 0.01024 nM) was used. Afterward, cell viability was determined using an MTS assay (MTS; Promega, Madison, WI). In brief, the MTS reagent (20 mL) was added to each well, followed by incubation at 37°C in a humidified, 5% CO_2 atmosphere for 2 h. Finally, the absorbance was read at 490 nm by using a Synergy 2 (BioTek, Winsooki, VT) plate reader. The cell viability was calculated as a percentage relative to control. Using cell viability percentage data under a series of drug concentrations, an individual IC_{50} value was calculated for each compound in each cell line. For a combination with two drugs, with a dose-response surface model based on the Bliss independence principle, interaction index (t) and its 95% CI were calculated to evaluate the two-drug combination effect.[23,24] When the tau is less than 1 and meanwhile the upper limit of its 95% CI is also less than 1, the combination effect of the two drugs is considered as significant synergism. This MTS assay was also used in further validation experiments.

Colony formation assay

SGC-996, GBC-SD, and NOZ cells were seeded onto six-well plates at a density of 5×10^2 cells per well and culture medium containing DMSO, gemcitabine, HKI-272, or a mixture of gemcitabine and HKI-272 was added and incubated for 2 weeks until clones were visible. Then cells were washed with PBS and fixed with methanol for 20 min, followed by staining with 0.1% crystal violet (Institute of Biotechnology) for 30 min at room temperature. Colonies were counted under an inverted microscope (IX71; Olympus Corporation, Tokyo, Japan).

Cell apoptosis assay

Cell apoptosis rate was assessed using YF®488-Annexin V/PI double staining Apoptosis Kit (US EVERBRIGHT INC., Sayreville, NJ). Briefly, 2 mL SGC-996, GBC-SD, and NOZ cells suspension were separately cultured in six-well plates (1×10^5 cells per well) and incubated in the presence of DMSO, gemcitabine, HKI-272, or a mixture of gemcitabine and HKI-272 for 48 h. Then these cells were harvested and washed twice using PBS and stained using binding buffer (500 µL) containing 5 µL PI and 5 µL YF®488-Annexin V for 15 min in the dark.[47] Finally, sample assessments were completed using a FACSCanto Flow Cytometer (BD Biosciences, San Jose, CA).

Cell cycle assay

A cell cycle assay was performed using PI staining (Beyotime, Shanghai, China). Cells treated with DMSO, gemcitabine, HKI-272, or a mixture of gemcitabine and HKI-272 were collected and washed twice in PBS. Then, cells are fixed in 75% ethanol at 4°C overnight. Last, cells are treated with RNase A, stained with PI, and analyzed by flow cytometry using MODFIT LT software (Verity Software House, Topsham, ME).

Cell migration and invasion assay

We used 8.0-µm pore trans-well plates (Corning, Corning, NY) to assess cell migration and invasion analysis which were carried out in a Matrigel invasion chamber (BD Biosciences) in a 24-well plate. SGC-996, GBC-SD, and NOZ cells were starved with serum-free medium for 24 h. Then the cells were harvested and seeded at a density of 2×10^4 cells per well in serum-free medium into the upper chamber, whereas we had added 500 µL complete medium to the lower chamber previously. In addition, DMSO, gemcitabine, HKI-272, or a mixture of gemcitabine and HKI-272 was added to both the upper and lower chambers. After incubation for 18 h at 37°C, cells on the upper chamber were swabbed off and the fixation of the cells on the lower surface with 4% paraformaldehyde was conducted for 15 min. Thereafter, 0.1% crystal violet staining was carried out for

Figure 7. EGFR activation is correlated with dismal prognosis and is an independent marker to survival in GBC

(A, B) Representative immunohistochemical and HE staining of EGFR expression in GBC clinical samples. (C) Kaplan-Meier curve of survival in GBC patients with high or low expression of EGFR. Patients with low EGFR expression exhibited longer life expectancy after surgery. (D) Gene-gene interaction (GGI) network for EGFR using GeneMania database. (E) PPI network for EGFR using the STRING database.

15 min. Finally, the invasive or migrated cell numbers were calculated in five random fields for each group.

Western blot analysis

Cells were lysed using protein extraction reagent (Biyuntian, Wuxi, China) supplemented with protease inhibitor cocktail (Calbiochem, San Diego, CA). Protein concentrations were determined with a BCA assay (Sigma, St. Louis, MO). Equal amounts of the extracts (30 mg/sample) were loaded and subjected to sodium dodecyl-sulfate polyacrylamide gel electrophoresis and transferred onto polyvinylidene fluoride membranes. Afterward, the membranes were blocked with blocking buffer, incubated overnight at 4°C with indicated primary antibodies, and then incubated with horseradish peroxidase-conjugated secondary antibodies. The detection was performed by ECL Supersignal West Pico Chemiluminescent Substrate. All antibodies used in this study were purchased from Cell Signaling Technology (Shanghai, China).

Ethics statement and *in vivo* experiments

Animal maintenance and experimental procedures were strictly performed following the guidelines of the Animal Care and Use Committee of Shanghai Jiao Tong University and approved by Institutional Animal Care & Use committee of Shanghai Jiao Tong University. A total of 5×10^5 luciferase-tagged GBC-SD human GBC cells stably expressing the firefly luciferase gene were subcutaneously transplanted into NOD/SCID mice (4–6 weeks old) of each group: group 1, control; group 2, gemcitabine (75 mg/kg, i.p., once weekly[48]); group 3, HKI-272 (40 mg/kg, p.o., once daily[49]); and group 4, gemcitabine plus HKI-272; n = 5 per group. Mice bearing luciferase-positive tumors were imaged by an IVIS 200 imaging system (Xenogen, Hopkinton, MA). Bioluminescent flux (photons/s/sr/cm$_2$) was determined for the primary tumors or lung metastasis. Besides, tumor size was also examined using an external caliper weekly and calculated based on the following equation: Volume = (length $\times$ width^2)/2.[50] At week 6, the body weights of each group of mice were obtained and both xenograft tumors and lungs metastases were carefully dissected out and pathologically confirmed as cancer tissue, followed by EGFR expression detection with both immunostaining and HE staining. All methods and experiments were carried out in accordance with the approved guidelines and regulations.

Immunohistochemical staining

A total of 131 GBC tissue samples were used for immunohistochemistry in our present study. All specimens from patients fixed in 10% buffered formalin were embedded in paraffin blocks. One slide from each specimen had been stained with HE and marked by a pathologist to ensure that the tissue section contained more than 80% tumor cells for macro-dissection. Consecutive 4-mm-thick sections were analyzed using a standard immunohistochemistry protocol and stained by antibodies of EGFR (Santa Cruz Biotechnology, Santa Cruz, CA). The scoring of immunohistochemistry is based on the staining intensity (I) and the proportion of stained quantity (q) of tumor cells to obtain a final score (Q) defined as the product of I $\times$ q and was performed by two independent pathologists. The scoring system for I was 0 = negative, 1 = low, 2 = moderate, and 3 = intense immunostaining; and for q was 0 = negative, 1 = 1%–9% positive, 2 = 10%–39% positive, 3 = 40%–69% positive, and 4 = 70%–100% positive cells.

HE staining

HE staining was conducted according to routine protocols.[51] Briefly, after deparaffinization and rehydration, 5-µm longitudinal sections were stained with hematoxylin solution for 5 min followed by five dips in 1% acid ethanol (1% HCl in 70% ethanol) and then rinsed in distilled water. Then the sections were stained with eosin solution for 3 min and followed by dehydration with graded alcohol and clearing in xylene. The mounted slides were then examined and photographed using an Olympus BX53 fluorescence microscope. The staining intensity was analyzed by software Image-Pro Plus 6.0.

Statistical analyses

All data are expressed as mean ± standard error of the mean. One-way ANOVA was used to determine the differences of cell viability, cell colony formation, cell apoptosis, cell cycle regulation, cell mobility and tumor size at week 6 between different groups. Repeated-measures ANOVA was used to determine tumor differences at various time points within one group of mice. Survival probabilities were determined using Kaplan-Meier analyses and compared by the log-rank test. Each experiment consisted of at least three replicates per condition. SPSS 19.0 software was used for all statistical analysis. A p value of less than 0.05 was considered statistically significant.

DATA AVAILABILITY STATEMENT

All data included in this study are available upon request by contact with the corresponding author.

SUPPLEMENTAL INFORMATION

Supplemental information can be found online at https://doi.org/10.1016/j.omto.2022.10.004.

AUTHOR CONTRIBUTIONS

D.Y. and J.W. conceived of the study and carried out its design. X.L., T.C., and J.H. performed the experiments. D.Y. and J.W. provided materials. D.Y. and T.C. analyzed the data. X.L. and D.Y. wrote and revised the manuscript with input from all authors. All authors read and approved the final manuscript.

DECLARATION OF INTERESTS

The authors declare no competing interests.

REFERENCES

1. Nara, S., Esaki, M., Ban, D., Takamoto, T., Shimada, K., Ioka, T., Okusaka, T., Ishii, H., and Furuse, J. (2020). Adjuvant and neoadjuvant therapy for biliary tract cancer: a review of clinical trials. Jpn. J. Clin. Oncol. 50, 1353–1363.

2. Bal, M.M., Ramadwar, M., Deodhar, K., and Shrikhande, S. (2015). Pathology of gallbladder carcinoma: current understanding and new perspectives. Pathol. Oncol. Res. 21, 509–525.

3. Sakata, J., Takizawa, K., Takano, K., Kobayashi, T., Minagawa, M., and Wakai, T. (2014). Current surgical treatment for gallbladder cancer. Nihon Geka Gakkai Zasshi 115, 185–189.

4. Ertel, A.E., Bentrem, D., and Abbott, D.E. (2016). Gall bladder cancer. Cancer Treat. Res. 168, 101–120.

5. Rakić, M., Patrlj, L., Kopljar, M., Kliček, R., Kolovrat, M., Loncar, B., and Busic, Z. (2014). Gallbladder cancer. Hepatobiliary Surg. Nutr. 3, 221–226.

6. Aloia, T.A., Járufe, N., Javle, M., Maithel, S.K., Roa, J.C., Adsay, V., Coimbra, F.J.F., and Jarnagin, W.R. (2015). Gallbladder cancer: expert consensus statement. HPB (Oxford) 17, 681–690.

7. Valle, J., Wasan, H., Palmer, D.H., Cunningham, D., Anthoney, A., Maraveyas, A., Madhusudan, S., Iveson, T., Hughes, S., Pereira, S.P., et al. (2010). Cisplatin plus gemcitabine versus gemcitabine for biliary tract cancer. N. Engl. J. Med. 362, 1273–1281.

8. Lamarca, A., Palmer, D.H., Wasan, H.S., Ross, P.J., Ma, Y.T., Arora, A., Falk, S., Gillmore, R., Wadsley, J., Patel, K., et al. (2021). Second-line FOLFOX chemotherapy versus active symptom control for advanced biliary tract cancer (ABC-06): a phase 3, open-label, randomised, controlled trial. Lancet Oncol. 22, 690–701.

9. Abdel-Rahman, O., Elsayed, Z., and Elhalawani, H. (2018). Gemcitabine-based chemotherapy for advanced biliary tract carcinomas. Cochrane Database Syst. Rev. 4, Cd011746.

10. Arteaga, C.L., and Engelman, J.A. (2014). ERBB receptors: from oncogene discovery to basic science to mechanism-based cancer therapeutics. Cancer Cell 25, 282–303.

11. Nakamura, H., Arai, Y., Totoki, Y., Shirota, T., Elzawahry, A., Kato, M., Hama, N., Hosoda, F., Urushidate, T., Ohashi, S., et al. (2015). Genomic spectra of biliary tract cancer. Nat. Genet. 47, 1003–1010.

12. Jiao, Y., Pawlik, T.M., Anders, R.A., Selaru, F.M., Streppel, M.M., Lucas, D.J., Niknafs, N., Guthrie, V.B., Maitra, A., Argani, P., et al. (2013). Exome sequencing identifies frequent inactivating mutations in BAP1, ARID1A and PBRM1 in intrahepatic cholangiocarcinomas. Nat. Genet. 45, 1470–1473.

13. Xu, M.J., Johnson, D.E., and Grandis, J.R. (2017). EGFR-targeted therapies in the post-genomic era. Cancer Metastasis Rev. 36, 463–473.

14. Razavi, P., Chang, M.T., Xu, G., Bandlamudi, C., Ross, D.S., Vasan, N., Cai, Y., Bielski, C.M., Donoghue, M.T.A., Jonsson, P., et al. (2018). The genomic landscape of endocrine-resistant advanced breast cancers. Cancer Cell 34, 427–438.e6.

15. Song, S.G., Kim, S., Koh, J., Yim, J., Han, B., Kim, Y.A., Jeon, Y.K., and Chung, D.H. (2021). Comparative analysis of the tumor immune-microenvironment of primary and brain metastases of non-small-cell lung cancer reveals organ-specific and EGFR mutation-dependent unique immune landscape. Cancer Immunol. Immunother. 70, 2035–2048.

16. Wu, M., and Zhang, P. (2020). EGFR-mediated autophagy in tumourigenesis and therapeutic resistance. Cancer Lett. 469, 207–216.

17. Yu, H.A., Suzawa, K., Jordan, E., Zehir, A., Ni, A., Kim, R., Kris, M.G., Hellmann, M.D., Li, B.T., Somwar, R., et al. (2018). Concurrent alterations in EGFR-mutant lung cancers associated with resistance to EGFR kinase inhibitors and characterization of MTOR as a mediator of resistance. Clin. Cancer Res. 24, 3108–3118.

18. Yang, D., Chen, T., Zhan, M., Xu, S., Yin, X., Liu, Q., Chen, W., Zhang, Y., Liu, D., Yan, J., et al. (2021). Modulation of mTOR and epigenetic pathways as therapeutics in gallbladder cancer. Mol. Ther. Oncolytics 20, 59–70.

19. Saura, C., Oliveira, M., Feng, Y.H., Dai, M.S., Chen, S.W., Hurvitz, S.A., Kim, S.B., Moy, B., Delaloge, S., Gradishar, W., et al. (2020). Neratinib plus capecitabine versus lapatinib plus capecitabine in HER2-positive metastatic breast cancer previously treated with ≥ 2 HER2-directed regimens: phase III NALA trial. J. Clin. Oncol. 38, 3138–3149.

20. Chan, A., Moy, B., Mansi, J., Ejlertsen, B., Holmes, F.A., Chia, S., Iwata, H., Gnant, M., Loibl, S., Barrios, C.H., et al. (2021). Final efficacy results of neratinib in HER2-positive hormone receptor-positive early-stage breast cancer from the phase III ExteNET trial. Clin. Breast Cancer 21, 80–91.e7.

21. Hyman, D.M., Piha-Paul, S.A., Won, H., Rodon, J., Saura, C., Shapiro, G.I., Juric, D., Quinn, D.I., Moreno, V., Doger, B., et al. (2018). HER kinase inhibition in patients with HER2- and HER3-mutant cancers. Nature 554, 189–194.

22. Li, M., Zhang, Z., Li, X., Ye, J., Wu, X., Tan, Z., Liu, C., Shen, B., Wang, X.A., Wu, W., et al. (2014). Whole-exome and targeted gene sequencing of gallbladder carcinoma identifies recurrent mutations in the ErbB pathway. Nat. Genet. 46, 872–876.

23. Harbron, C. (2010). A flexible unified approach to the analysis of pre-clinical combination studies. Stat. Med. 29, 1746–1756.

24. Liu, Q., Yin, X., Languino, L.R., and Altieri, D.C. (2018). Evaluation of drug combination effect using a Bliss independence dose-response surface model. Stat. Biopharm. Res. 10, 112–122.

25. Chen, H., Zhou, L., Wu, X., Li, R., Wen, J., Sha, J., and Wen, X. (2016). The PI3K/AKT pathway in the pathogenesis of prostate cancer. Front. Biosci. 21, 1084–1091.

26. Wu, T.K., Ou, Y.C., Chen, Y.P., Huang, F.M., Pan, Y.R., and Lee, C.J. (2021). Cetyltrimethylammonium bromide attenuates the mesenchymal characteristics of hypopharyngeal squamous cell carcinoma through inhibiting the EGFR/PI3K/AKT signaling pathway. Anticancer Res. 41, 3789–3799.

27. Lee, M.M.L., Chan, B.D., Wong, W.Y., Qu, Z., Chan, M.S., Leung, T.W., Lin, Y., Mok, D.K.W., Chen, S., and Tai, W.C.S. (2020). Anti-cancer activity of centipeda minima extract in triple negative breast cancer via inhibition of AKT, NF-κB, and STAT3 signaling pathways. Front. Oncol. 10, 491.

28. Sun, Y., He, J., Shi, D.B., Zhang, H., Chen, X., Xing, A.Y., and Gao, P. (2021). Elevated ZBTB7A expression in the tumor invasive front correlates with more tumor budding formation in gastric adenocarcinoma. J. Cancer Res. Clin. Oncol. 147, 105–115.

29. Kuipers, H., de Bitter, T.J.J., de Boer, M.T., van der Post, R.S., Nijkamp, M.W., de Reuver, P.R., Fehrmann, R.S.N., and Hoogwater, F.J.H. (2021). Gallbladder cancer: current insights in genetic alterations and their possible therapeutic implications. Cancers (Basel) 13, 5257.

30. Sharma, A., Kumar, A., Kumari, N., Krishnani, N., and Rastogi, N. (2017). Mutational frequency of KRAS, NRAS, IDH2, PIK3CA, and EGFR in North Indian gallbladder cancer patients. Ecancermedicalscience 11, 757.

31. Wang, R., Godet, I., Yang, Y., Salman, S., Lu, H., Lyu, Y., Zuo, Q., Wang, Y., Zhu, Y., Chen, C., et al. (2021). Hypoxia-inducible factor-dependent ADAM12 expression mediates breast cancer invasion and metastasis. Proc. Natl. Acad. Sci. USA 118. e2020490118.

32. Yang, L.P., Yang, Z.L., Tan, X.G., and Miao, X.Y. (2010). Expression of annexin A1 (ANXA1) and A2 (ANXA2) and its significance in benign and malignant lesions of gallbladder. Zhonghua Zhong Liu Za Zhi 32, 595–599.

33. Valle, J.W., Kelley, R.K., Nervi, B., Oh, D.Y., and Zhu, A.X. (2021). Biliary tract cancer. Lancet 397, 428–444.

34. Nemunaitis, J.M., Brown-Glabeman, U., Soares, H., Belmonte, J., Liem, B., Nir, I., Phuoc, V., and Gullapalli, R.R. (2018). Gallbladder cancer: review of a rare orphan gastrointestinal cancer with a focus on populations of New Mexico. BMC cancer 18, 665.

35. Boutros, C., Gary, M., Baldwin, K., and Somasundar, P. (2012). Gallbladder cancer: past, present and an uncertain future. Surg. Oncol. 21, e183–e191.

36. Choi, I.S., Kim, K.H., Lee, J.H., Suh, K.J., Kim, J.W., Park, J.H., Kim, Y.J., Kim, J.S., Kim, J.H., and Kim, J.W. (2021). A randomised phase II study of oxaliplatin/5-FU (mFOLFOX) versus irinotecan/5-FU (mFOLFIRI) chemotherapy in locally advanced or metastatic biliary tract cancer refractory to first-line gemcitabine/cisplatin chemotherapy. Eur. J. Cancer 154, 288–295.

37. Zheng, S., Wang, X., Fu, Y., Li, B., Xu, J., Wang, H., Huang, Z., Xu, H., Qiu, Y., Shi, Y., and Li, K. (2021). Targeted next-generation sequencing for cancer-associated gene mutation and copy number detection in 206 patients with non-small-cell lung cancer. Bioengineered 12, 791–802.

38. Hosomi, Y., Morita, S., Sugawara, S., Kato, T., Fukuhara, T., Gemma, A., Takahashi, K., Fujita, Y., Harada, T., Minato, K., et al. (2020). Gefitinib alone versus Gefitinib plus chemotherapy for non-small-cell lung cancer with mutated epidermal growth factor receptor: NEJ009 study. J. Clin. Oncol. 38, 115–123.

39. Neal, J.W., Costa, D.B., Muzikansky, A., Shrager, J.B., Lanuti, M., Huang, J., Ramachandran, K.J., Rangachari, D., Huberman, M.S., Piotrowska, Z., et al. (2021). Randomized phase II study of 3 Months or 2 Years of adjuvant Afatinib in patients with surgically resected stage I-III EGFR-mutant non-small-cell lung cancer. JCO Precis. Oncol. 5, 325–332.

40. Rizvi, N.A., Hellmann, M.D., Brahmer, J.R., Juergens, R.A., Borghaei, H., Gettinger, S., Chow, L.Q., Gerber, D.E., Laurie, S.A., Goldman, J.W., et al. (2016). Nivolumab in combination with platinum-based doublet chemotherapy for first-line treatment of advanced non-small-cell lung cancer. J. Clin. Oncol. 34, 2969–2979.

41. Cerami, E., Gao, J., Dogrusoz, U., Gross, B.E., Sumer, S.O., Aksoy, B.A., Jacobsen, A., Byrne, C.J., Heuer, M.L., Larsson, E., et al. (2012). The cBio cancer genomics portal: an open platform for exploring multidimensional cancer genomics data. Cancer Discov. 2, 401–404.

42. Gao, J., Aksoy, B.A., Dogrusoz, U., Dresdner, G., Gross, B., Sumer, S.O., Sun, Y., Jacobsen, A., Sinha, R., Larsson, E., et al. (2013). Integrative analysis of complex cancer genomics and clinical profiles using the cBioPortal. Sci. Signal. 6, pl1.

43. Li, T., Fan, J., Wang, B., Traugh, N., Chen, Q., Liu, J.S., Li, B., and Liu, X.S. (2017). TIMER: a web server for comprehensive analysis of tumor-infiltrating immune cells. Cancer Res. 77, e108–e110.

44. Yang, W., Soares, J., Greninger, P., Edelman, E.J., Lightfoot, H., Forbes, S., Bindal, N., Beare, D., Smith, J.A., Thompson, I.R., et al. (2013). Genomics of Drug Sensitivity in Cancer (GDSC): a resource for therapeutic biomarker discovery in cancer cells. Nucleic Acids Res. 41, D955–D961.

45. Warde-Farley, D., Donaldson, S.L., Comes, O., Zuberi, K., Badrawi, R., Chao, P., Franz, M., Grouios, C., Kazi, F., Lopes, C.T., et al. (2010). The GeneMANIA predic-tion server: biological network integration for gene prioritization and predicting gene function. Nucleic Acids Res. 38, W214–W220.

46. Szklarczyk, D., Gable, A.L., Nastou, K.C., Lyon, D., Kirsch, R., Pyysalo, S., Doncheva, N.T., Legeay, M., Fang, T., Bork, P., et al. (2021). The STRING database in 2021: customizable protein-protein networks, and functional characterization of user-uploaded gene/measurement sets. Nucleic Acids Res. 49, D605–D612.

47. Teng, J.F., Qin, D.L., Mei, Q.B., Qiu, W.Q., Pan, R., Xiong, R., Zhao, Y., Law, B.Y.K., Wong, V.K.W., Tang, Y., et al. (2019). Polyphyllin VI, a saponin from Trillium tschonoskii Maxim. induces apoptotic and autophagic cell death via the ROS triggered mTOR signaling pathway in non-small cell lung cancer. Pharmacol. Res. 147, 104396.

48. Fotopoulou, C., Baumunk, D., Schmidt, S.C., and Schumacher, G. (2010). Additive growth inhibition after combined treatment of 2-methoxyestradiol and conventional chemotherapeutic agents in human pancreatic cancer cells. Anticancer Res. 30, 4619–4624.

49. Rabindran, S.K., Discafani, C.M., Rosfjord, E.C., Baxter, M., Floyd, M.B., Golas, J., Hallett, W.A., Johnson, B.D., Nilakantan, R., Overbeek, E., et al. (2004). Antitumor activity of HKI-272, an orally active, irreversible inhibitor of the HER-2 tyrosine kinase. Cancer Res. 64, 3958–3965.

50. Tomayko, M.M., and Reynolds, C.P. (1989). Determination of subcutaneous tumor size in athymic (nude) mice. Cancer Chemother. Pharmacol. 24, 148–154.

51. Guo, Y., Wang, L., Ma, R., Mu, Q., Yu, N., Zhang, Y., Tang, Y., Li, Y., Jiang, G., Zhao, D., et al. (2016). JiangTang XiaoKe granule attenuates cathepsin K expression and improves IGF-1 expression in the bone of high fat diet induced KK-Ay diabetic mice. Life Sci. 148, 24–30.